JOURNAL OF MOLECULAR SPECTROSCOPY 123, 340–355 (1987)

Submillimeter-Wave Spectrum and Spectroscopic Constants of AsH_3 in the (0100) and (0001) Vibrational States and Joint Analysis of Submillimeter and Infrared Data

V. P. KAZAKOV,* A. F. KRUPNOV,* V. N. SAVELIEV,† AND O. N. ULENIKOV†

*Institute of Applied Physics, Academy of Sciences of the USSR, Gorky 603600, and †Institute of Atmospheric Optics, Siberian Branch USSR Academy of Sciences, Tomsk 634055, USSR

The submillimeter-wave spectra of the arsine molecule in the excited vibrational states (0100) and (0001) have been investigated for both allowed R branches ($J + 1 \leftarrow J$, $K \leftarrow K$) and weak-intensity "forbidden" Q branches ($K = 3 \leftarrow 1$, $3 \leftarrow 0$, $2 \leftarrow 0$). Weak "forbidden" transitions of the AsH_3 molecule in the (0001) state can be observed due to the increase of sensitivity of a RAD-spectrometer by using quasi-optical cavity absorption cells. As a result of joint analysis of new submillimeter recordings together with the known infrared, microwave, and radiofrequency data, the set of spectroscopic parameters obtained allows one to describe all the available spectroscopic data for the (0100) and (0001) vibrational states of the AsH_3 molecule within experimental uncertainties.

I. INTRODUCTION

In preceding papers (*1, 2*) it was noted that the rotational spectrum of the XH_3 symmetric top molecules, where X = N, P, in excited vibrational states, is a subject of extensive research, in particular because of problems connected with the presence of strong Coriolis interactions, the possibility of observing the "forbidden" ($\Delta K \neq 0$) spectra, and in view of the important role which such molecules play in many fields of physics, chemistry, and astronomy. In earlier studies (*3, 4*), the "forbidden" spectrum $\Delta K = 3$ in the submillimeter-wave region was observed for the NH_3 and PH_3 molecules. The rotational spectrum of a light symmetric top molecule AsH_3 is located in short-millimeter- and submillimeter-wave spectral regions and that makes their experimental study difficult, especially with high microwave resolution and accuracy. Moreover, it is difficult to investigate the arsine spectrum because of (1) the small ($\mu = 0.22$ D, Ref. (*5*)) dipole moment of this molecule, which leads to low intensities of not only its "forbidden" but even its allowed spectra, and (2) the quadrupole interaction of the As nucleus with the molecular field, which results in significant (on the order of ~ 100 MHz) splittings of vibration–rotation levels and the very complex appearance of the observed spectra.

The AsH_3 submillimeter-wave spectrum in the ground vibrational state was investigated in Ref. (*6*). For the excited vibrational states it is necessary to take into account strong interactions, e.g., between the (0100) and (0001) states. So a combined analysis of precise data obtained in different spectral regions cannot always be successful. This paper is aimed at, on the one hand, the experimental investigation of submillimeter-wave rotational spectra of the excited states (0100) and (0001) of the arsine molecule,

0022-2852/87 $3.00

including the weak "forbidden" transitions, and, on the other, the correct analysis of its high- and superhigh-resolution spectra taking into account the interactions between the (0100) and (0001) states, including the presence of accidental resonances. The observation of "forbidden" spectra would give, in this case, information which could not be obtained from conventional allowed spectra of molecules with such symmetry characteristics. The difficulties in predicting the location of submillimeter-wave "forbidden" lines in the excited states require a search in a wide continuous range of frequencies with high sensitivity. To satisfy these requirements we used a scanning submillimeter-microwave spectrometer RAD equipped with quasi-optical cavity cells (*8, 9*). The details of the experimental investigations carried out, the procedure of measurements, and the results obtained are described in Section II. Sections III and IV deal with the theoretical background and the analysis of the experimental data on fine and hyperfine structure of spectra in the bands ν_2 and ν_4.

II. EXPERIMENTAL DETAILS AND THE ROTATIONAL SPECTRUM OF THE AsH_3 MOLECULE

The rotational spectrum of the arsine molecule was investigated in the frequency range 200–940 GHz using a scanning submillimeter spectrometer RAD with a system intended for accurate frequency measurements (*10*). To observe weak lines, high-purity samples supplied by the Institute of Chemistry, Gorky, were used. The absorption coefficients of electric dipole transitions caused by centrifugal distortion in the excited vibrational states as well as of the transitions $\Delta K = 3$ in the ground state (*6*) are very small ($\sim 10^{-7}$–10^{-8} cm^{-1}) in the submillimeter-frequency region of interest. To observe these weak lines, the submillimeter spectrometer sensitivity was increased by the use of two types of quasi-optical resonator absorption cells in the form of a closed cylindrical metallic cavity (*8, 9*). As a result, the sensitivity, corresponding to the minimum absorption detectable coefficient ($S/N = 1$), $\gamma_{min} = (60 - 3)10^{-11}$ cm^{-1}, was achieved in the frequency range 200–380 GHz at a mean power of radiation source of ~ 10 mW and a time constant of ~ 1 sec.

All measurements of both allowed and "forbidden" transitions were carried out at room temperature at comparatively high pressures ($P = 0.2$–0.7 Torr). It was difficult to make high-accuracy measurements of the line center frequencies in the AsH_3 states (0100) and (0001) because of the influence of wings of adjacent hyperfine quadrupole components, especially for the transitions of the R branch $J = 2 \leftarrow 1$. Under such conditions the measurement accuracy was limited to ~ 300 kHz excluding the case of hyperfine structure of the transitions $J = 1 \leftarrow 0$ in the (0100) and (0001) states. Examples of recordings of the rotational spectrum of the transitions $J = 4 \leftarrow 3$ in the (0100) and (0001) states are given in Figs. 1 and 2, respectively (see also Table VIII). The accuracy of the line centers is about 5–7 MHz for the region near 860 GHz and about 15–25 MHz for the region near 920 GHz. Such recordings, which were made with an unstabilized source of radiation and with relatively low resolution, allow one to obtain only the K and K, l-structures of transitions (Figs. 1 and 2).

Twenty-one transitions of R branches ($J + 1 \leftarrow J$, $K \leftarrow K$, $\Delta F = 0, \pm 1$, see Table I) and 20 frequencies of hyperfine quadrupole components of the "forbidden" transitions of Q branches ($J \leftarrow J$, $\Delta F = 0$, $K = 3 \leftarrow 1$, $3 \leftarrow 0$, $2 \leftarrow 0$, see Table II) were observed and measured in the AsH_3 excited vibrational states (0100) and (0001).

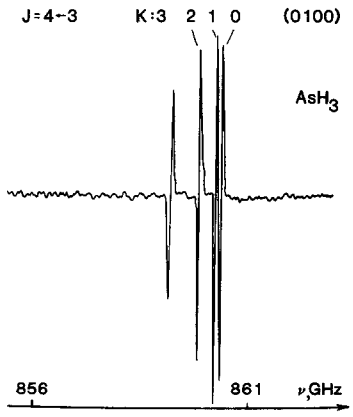

FIG. 1. Recording of K structure of the transition $J = 4 \leftarrow 3$ in the (0100) vibrational state of the AsH_3 molecule. The lines are recorded in the form of derivatives of absorption profiles.

The "perturbation allowed" spectrum of the AsH_3 molecule was investigated in the frequency region 320–380 GHz. Figure 3 gives a sample of the observed rotational spectrum of hyperfine quadrupole components of "forbidden" transitions of the Q branch ($K = 3 \leftarrow 1$, $J = 5$ and $K = 3 \leftarrow 0$, $J = 8$).

During early investigations of AsH_3 millimeter- and submillimeter-wave spectra in the (0100) and (0001) states only the low-resolution data from Ref. (*1*) were available. The recording and assignment of the AsH_3 weak transitions caused by centrifugal distortion in the excited states were based on the properties typical for the AsH_3 molecule because the available data would not allow one to accurately predict frequencies of such transitions. In the Q branches of AsH_3 only four intense adjacent hyperfine components ($J \leftarrow J$, $\Delta F = 0$) were observed. The dependence of frequency intervals between both the doublets and the hyperfine components inside the doublets has been observed for AsH_3. Thus, each rotational quantum number J corresponds to an individual location of hyperfine components whose behavior can be estimated using, e.g., information from Ref. (*12*). Search of the lines with typical quadrupole splitting

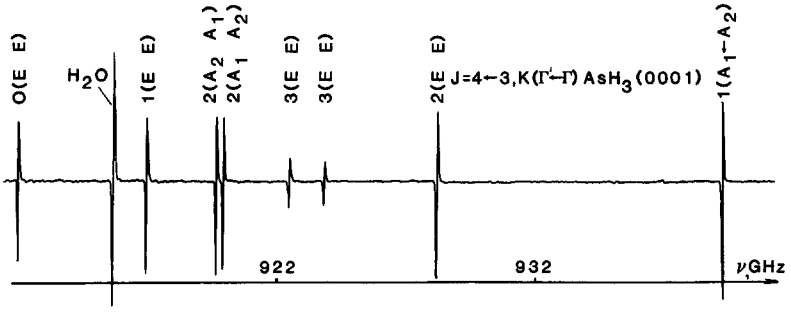

FIG. 2. Recording of K, l structure of the transition $J = 4 \leftarrow 3$ in the (0001) vibrational state of the AsH_3 molecule. A line of the transition $4_{22} \leftarrow 3_{31}$ of the $H_2{}^{16}O$ molecule is indicated by the arrow.

TABLE I

Transition Frequencies of the AsH_3 Molecule in the (0100) and (0001) Vibrational States: Allowed Transitions $J + 1 \leftarrow J$ ($\Delta K = 0$)[a]

Transition K Γ F′ ← F	Exp., MHz	Calc., MHz	E.-C., KHz
(0100)	J = 1 ← 0 , Ref.(11)		
0 A1 3/2-3/2	214 725.85	214 725.865	- 15
5/2-3/2	214 766.07	214 766.085	- 15
1/2-3/2	214 797.65	214 797.690	30
(0100)	J = 2 ← 1		
1 E 5/2-3/2	429 569.81	429 569.453	357
5/2-5/2	429 589.32	429 589.323	- 3
7/2-5/2	429 609.92	429 609.977	- 59
3/2-1/2	429 619.72	429 620.084	-362
0 A2 5/2-5/2	429 634.34	429 634.601	-263
5/2-3/2	429 675.01	429 674.821	190
7/2-5/2	429 675.01	429 675.050	- 39
3/2-3/2	429 703.29	429 703.179	112
(0001)	J = 1 ← 0 , Ref.(11)		
0 E 3/2-3/2	230 562.18	230 562.187	- 7
5/2-3/2	230 602.28	230 602.299	- 19
1/2-3/2	230 633.69	230 633.664	26
(0001)	J = 2 ← 1		
1 E 5/2-3/2	461 225.16	461 225.324	-164
5/2-5/2	461 245.13	461 244.954	178
7/2-5/2	461 265.24	461 265.200	40
3/2-1/2	461 275.16	461 275.240	- 56
1 A2 5/2-3/2	470 481.10	470 481.378	- 278
5/2-5/2	470 501.44	470 501.222	218
7/2-5/2	470 521.31	470 521.460	-150
3/2-1/2	470 531.89	470 531.674	216

[a] Here and in Tables II–IV, VI, and VIII–X, Γ is the symmetry of the lower rotation–vibration state.

between the pairs of blending doublets was carried out based on the survey recordings which were made in a wide region of submillimeter frequencies at different pressures. Then a hyperfine structure of the rotational transitions typical for AsH_3 (Fig. 3) was observed by a frequency-measuring system. Such a procedure was successfully applied for searching for weak "forbidden" transitions $\Delta K = 3$ of AsH_3 in the ground state (*6*). The additional criterion of assignment of the "forbidden" transitions in the (0001) state was a temperature-dependent behavior of the intensities of the lines.

One of the aims of the present paper is the investigation of the "perturbation allowed" transitions including those which have not been observed earlier in the microwave spectra ($\Delta K = 2$). Moreover, the spectrum of regular transitions in the R branch is also studied since there are no microwave submillimeter data on the AsH_3 (0100) and

TABLE II

Transition Frequencies of the AsH_3 Molecule in the (0001) Vibrational State: "Forbidden" Transitions $J \leftarrow J$ ($\Delta K = 2$, $\Delta K = 3$), $\Gamma = E$

Transition J F′ ← F	Exp., MHz	Calc., MHz	E.-C., KHz
	K = 3 ← 1		
5 7/2- 7/2	323 401.54	323 401.422	118
13/2-13/2	323 409.79	323 409.614	176
9/2- 9/2	323 430.42	323 430.579	-159
11/2-11/2	323 438.66	323 438.794	-134
6 9/2- 9/2	346 601.80	346 601.766	34
15/2-15/2	346 606.79	346 606.718	72
11/2-11/2	346 622.72	346 622.740	- 20
13/2-13/2	346 627.61	346 627.696	- 86
7 11/2-11/2	380 785.52	380 785.317	203
17/2-17/2	380 790.77	380 790.685	85
13/2-13/2	380 811.60	380 811.722	-122
15/2-15/2	380 816.93	380 817.096	-166
	K = 3 ← 0		
8 13/2-13/2	328 946.97	328 947.069	- 99
19/2-19/2	328 950.69	328 950.659	31
15/2-15/2	328 967.23	328 967.193	- 37
17/2-17/2	328 970.82	328 970.788	32
	K = 2 ← 0		
8 13/2-13/2	350 499.96	350 500.111	-151
19/2-19/2	350 503.75	350 503.761	- 11
15/2-15/2	350 520.70	350 520.577	123
17/2-17/2	350 524.27	350 524.232	38

(0001) excited states. The results of our experimental studies of the AsH_3 molecule in the (0100) and (0001) vibrational states together with the earlier microwave data (*7, 11, 13*) are presented in Tables I–IV.

The estimation of the absorption coefficients of the investigated "forbidden" transitions in the (0001) state, in comparison with, e.g., the "forbidden" transitions $\Delta K = 3$ in the (0000) state or with the known weak lines in the excited vibrational states (001), (200), and (040) of the N_2O molecule, is also of particular interest. Thus, using a spectrometer RAD with a quasi-optical resonator absorption cell with sensitivity $\gamma_{min} = 3 \cdot 10^{-11}$ cm^{-1} (*9*), it was found that for the "forbidden" transitions of the Q branches in the (0001) state ($K = 3 \leftarrow 0$, $J = 8$ and $K = 3 \leftarrow 1$, $J = 5$) the total absorption coefficient is, respectively, ~7 and ~5 times larger than that of the transition $\Delta K = 3$ ($K = 6 \leftarrow 9$, $J = 11$) of AsH_3 in the (0000) state, whereas the total absorption coefficient of the allowed transition of the R branch $J = 1 \leftarrow 0$ in the (0001) state is ~240 times smaller than that of the similar transition $J = 1 \leftarrow 0$ in the (0000) state. The data on the rotational "forbidden" transition intensities can be useful for deter-

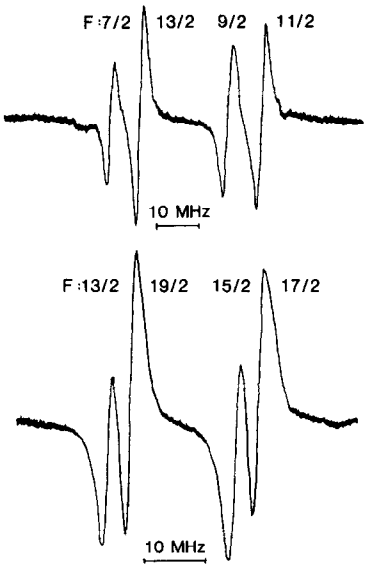

FIG. 3. Recordings of the submillimeter-wave spectrum of the Q branches: $K = 3 \leftarrow 1$, $J = 5$ and $K = 3 \leftarrow 0$, $J = 8$ in the (0001) vibrational state of the AsH_3 molecule obtained at the quasi-optical cavity cell RAD.

mining the dipole moment of the AsH_3 molecule. These experimental measurements and the corresponding theoretical estimations will be presented in detail in a subsequent paper.

III. THEORETICAL BACKGROUND

The AsH_3 molecule is one of the symmetric top molecules with C_{3v} symmetry and has been extensively investigated in spectroscopy during previous years. However, the theoretical analysis of the AsH_3 fine and hyperfine structures is very complicated as a result of a very strong interaction of the As nuclear quadrupole moment with the intramolecular electric field, as well as strong Coriolis interactions. In particular, the separation between the energy levels of the vibrational states (0100) and (0001) considered in the present paper is only 90 cm^{-1}, and the resonance Coriolis interaction is determined by the value $\sim C_{11}(2J(J+1) - 2K(K+1))^{1/2}$, where $C_{11} \approx 1.9$ cm^{-1} (*2*). Therefore, the centers of spectral lines even for small values of rotational quantum numbers J and K can be shifted strongly and the spectra cannot be described using simple mathematical models. For example, in spite of the results of Ref. (*2*), where the fine structures of the ν_2 and ν_4 infrared bands have been described, taking into account the Coriolis interaction, the hyperfine quadrupole structure of direct l-type doubling transitions in the (0001) state of AsH_3 ($J = 6, 7, 8$) has not been described in Ref. (*7*). It should also be noted that the parameters obtained, e.g., in Refs. (*1, 2, 7, 11, 13*), which describe the experimental data in one of the spectral regions, do not predict the centers of the lines in the other spectral regions within the experimental accuracy.

TABLE III

Values of Transition Frequencies of Direct *l*-Type Doubling Transitions in the (0001) Vibrational State ($K = 1 \leftarrow 1$) of AsH_3[a]

Transition J Γ F′ ← F	Exp., MHz	Calc., MHz	E.-C., KHz
1 A1 5/2- 5/2	9 772.06	9 772.049	11
1/2- 3/2	9 736.20	9 736.212	- 12
5/2- 3/2	9 752.84	9 752.812	28
3/2- 5/2	9 791.83	9 791.888	- 58
3/2- 1/2	9 808.03	9 807.999	31
2 A2 1/2- 1/2	29 060.50	29 060.471	29
7/2- 7/2	29 060.98	29 060.901	79
5/2- 5/2	29 061.49	29 061.506	- 16
1/2- 3/2	29 080.68	29 080.709	- 29
7/2- 5/2	29 081.74	29 081.744	- 4
3/2- 5/2	29 075.34	29 075.358	- 18
5/2- 3/2	29 047.24	29 047.223	17
5/2- 7/2	29 040.72	29 040.663	57
3/2- 1/2	29 040.72	29 040.836	-116
3 A1 3/2- 3/2	57 380.61	57 380.179	431[b]
5/2- 5/2		57 380.769	-159
7/2- 7/2		57 381.044	-434[b]
9/2- 9/2		57 380.451	159
6 A2 9/2- 9/2	188 858.44	188 858.141	299
15/2-15/2		188 858.405	35
11/2-11/2	188 859.35	188 859.376	- 26
13/2-13/2		188 859.658	-308
7 A1 11/2-11/2	244 525.68	244 525.442	238
17/2-17/2		244 525.867	-187
13/2-13/2	244 527.83	244 527.635	195
15/2-15/2		244 528.075	-245
8 A2 13/2-13/2	303 312.70	303 312.674	25
19/2-19/2	303 313.52	303 313.595	- 75
15/2-15/2	303 317.79	303 317.694	96
17/2-17/2	303 318.53	303 318.576	- 46

[a] The experimental data are taken from Ref. (*7*).
[b] These two values were not used in the fitting.

Therefore, in the present paper an attempt has been made to obtain a set of parameters for simultaneous description, with the accuracy close to experimental values, of all modern data for the (0100) and (0001) vibrational states of AsH_3 (both infrared (*2*) and direct *l*-type doubling transitions (*7*) (Table III), radiofrequency transitions (*13*) (Table IV), and allowed (Table I) and "forbidden" (Table II) transitions in the submillimeter-wave region).

TABLE IV

Radiofrequency Transitions in the (0100) and (0001) Vibrational States of AsH_3

Transition J Γ K	F′ ← F	Exp., MHz	Calc., MHz	E.-C., KHz
		(0100)		
5 5 E	11/2- 9/2	17.475	17.489	-14
	11/2-13/2	59.240	59.231	9
	9/2- 7/2	60.406	60.405	1
6 5 E	13/2-11/2	8.105	8.085	20
	13/2-15/2	30.473	30.461	12
	11/2- 9/2	31.832	31.852	-20
		(0001)		
5 5 E	11/2- 9/2	17.388	17.382	6
	11/2-13/2	58.486	58.487	- 1

The same Hamiltonian as in Ref. (*2*) was used for describing the values of the centers of quadrupole multiplets. In this case the diagonal matrix elements of the Hamiltonian have the form

$$E_v(J,k,l) = G_v + B_v[J(J+1)-k^2] + C_v k^2 - 2(C\xi)_v kl - D_J^v J^2(J+1)^2 - D_{JK}^v J(J+1)k^2$$
$$- D_K^v k^4 + \eta_{vJ} J(J+1)kl + \eta_{vK} k^3 l + H_J^v J^3(J+1)^3 + H_{JK}^v J^2(J+1)^2 k^2$$
$$+ H_{KJ}^v J(J+1)k^4 + H_K^v k^6 + \tau_{vJ} J^2(J+1)^2 kl + \tau_{vJK} J(J+1)k^3 l + \tau_{vK} k^5 l + \tau_{vK}^* k^3 l^3. \quad (1)$$

Here, as in Ref. (*2*), $v = 4$, $l = 1$ or $v = 2$, $l = 0$. Nondiagonal matrix elements were used in the same form as in Ref. (*2*) (see Table II of (*2*)).

The existence of the nuclear spin $I = \frac{3}{2}$ of the As nucleus leads to splitting of each level (*14*), defined by Eq. (1) and the corresponding nondiagonal matrix elements $\langle v_2 v_4^l JK| \cdots |\tilde{v}_2 \tilde{v}_4^{\tilde{l}} J\tilde{K}\rangle$ from Table II of Ref. (*2*), into four hyperfine components (see Fig. 4). This splitting is determined by the formula (*14–16*)

$$W_v^{\pm}(F,J,K) = \left\{[(eqQ)^v + \chi_J^v J(J+1) + \chi_K^v K^2]\cdot\left[\frac{3K^2}{J(J+1)} - 1 \pm \eta^v\right] + \chi_d^v \frac{K^2(4K^2-1)}{J(J+1)}\right\}$$
$$\times f(I,F,J) + \frac{1}{2}\left[C_N^v + (C_K^v - C_N^v)\frac{K^2}{J(J+1)}\right]\cdot[F(F+1) - I(I+1) - J(J+1)]. \quad (2)$$

Here $K = |k|$, $I = \frac{3}{2}$, and $F = J \pm \frac{1}{2}$ or $J \pm \frac{3}{2}$. The small parameter η^v in Eq. (*2*) is nonzero for $v = 4$ only ($\eta^{v=2} = 0$), and it is a measure of the asymmetry of the electric field gradient produced by the degenerate vibration q_4 (see (*16*)). In this case, the sign "+" or "−" refers to the symmetric or antisymmetric components of the *l*-type doublet, respectively (*20*). Function $f(I, F, J)$ is the known Casimir function (*14*) and all the designations of the parameters in Eq. (2) have the standard meanings: $(eqQ)^v$ are the

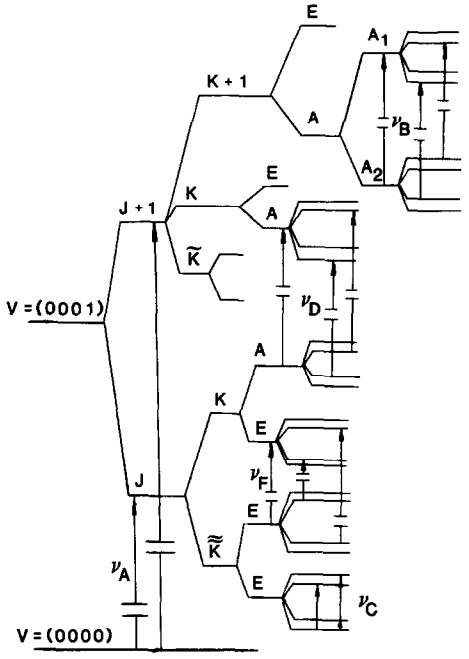

FIG. 4. Energy levels and transition types in the AsH_3 molecule.

effective quadrupole coupling constants; χ_J^v and χ_K^v are the coefficients of their rotational dependence; χ_d^v are the Hougen distortion coefficients (*15*); and C_N^v and C_K^v are the magnetic spin–rotation coupling constants.

It should be noted that formula (2), which is suitable for describing the quadrupole hyperfine splitting in noninteracting vibrational states, is not suitable for strong interacting states. Such a situation occurs for the (0100) and (0001) states of the AsH_3 molecule. In particular, as was mentioned earlier, the use of formula (2) proved unsuccessful for describing hyperfine quadrupole structures of the direct *l*-type doubling transitions ($v_4 = 1$, $J = 6, 7, 8$) in Ref. (*7*).

For describing the experimental fine and hyperfine energy structures of the (0100) and (0001) vibrational states, both recorded by us and known before, we have used the expression analogous to Eq. (34) of Ref. (*17*), which was obtained using the following procedure.

Let the wavefunctions of vibration–rotation states have the form

$$\psi_{\tilde{v}J\tilde{K}} = \sum_{v=2,4} \sum_{K} \alpha_{vJK}^{\tilde{v}\tilde{K}} |v\rangle |JK\rangle. \tag{3}$$

Here the presence of nonzero coefficients $\alpha_{vJK}^{\tilde{v}\tilde{K}}$ at $\tilde{v} \neq v$ in the right-hand side of Eq. (3) corresponds to the presence of Coriolis resonance interaction between the (0100) and (0001) states. Then, if one uses these wavefunctions and makes transformations as in, e.g., Refs. (*14, 15*) for obtaining formula (2), one can show that Eq. (2) will be transformed to

$$\tilde{W}_{\tilde{v}}^{\pm}(F,J,K) = \sum_{vK} (\alpha_{vJK}^{\tilde{v}\tilde{K}})^2 W_v^{\pm}(F,J,K), \tag{4}$$

where $W_v^{\pm}(F, J, K)$ are the values from Eq. (2).

It should be noted that the main part of $W_v^{\pm}(F, J, K)$ has the form

$$(eqQ)^v\left\{\frac{3K^2}{J(J+1)}-1\right\}\cdot f(I,F,J),$$

that is, it depends strongly on the quantum number K. But, as is known, the Coriolis interaction connects states $|JK\rangle$ with different K values in the wavefunctions of Eq. (3). So, the Coriolis interaction must lead to strong changes in hyperfine splitting obtained by Eq. (4) in comparison with the nonresonance situation of Eq. (2).

IV. ANALYSIS OF EXPERIMENTAL DATA

The analysis of experimental data (fine structure of IR bands ν_2 and ν_4 (*2*), transitions of *A*-type in Fig. 4; direct *l*-type doubling transitions (*7*), *B*-type; radiofrequency transitions (*13*), *C*-type; and the data from Tables I–II, *D*- and *F*-types) was made in three steps. First, on the basis of rotational, centrifugal, and resonance parameters for the (0100) and (0001) states from Ref. (*2*), the vibration–rotation wavefunctions of $\psi_{\tilde{v}J\tilde{K}}$-type (see Eq. (3)) were obtained. Then, the coefficients $\alpha_{vJK}^{\tilde{v}\tilde{K}}$ from this wavefunction were used in Eq. (4), and the dependences of the values $\tilde{W}_{\tilde{v}}^{\pm}(F, J, K)$ on the parameters $(eqQ)^v$, χ_J^v, χ_K^v, χ_d^v, C_N^v, C_K^v, and $\eta^{v=4}$ were obtained. In this case, because of smallness of the terms $\chi_J^4\cdot J(J+1)\cdot\eta$ and $\chi_K^4\cdot K^2\cdot\eta$ in comparison with $(eqQ)^4\cdot\eta$, these first two terms have been omitted in $W_v^{\pm}(F, J, K)$. As a consequence, both the expressions obtained for $\tilde{W}_{\tilde{v}}^{\pm}(F, J, \tilde{K})$ (Eq. (4)) and the expressions for the line center frequencies from Tables I–IV became linear to the parameters $(eqQ)^v, \chi_J^v, \ldots, (eqQ)^4\cdot\eta$. It should be noted that besides the above parameters, the "centers" of quadrupole multiplets (ν_B, ν_D, or ν_F in Fig. 4) are linearly presented in the expressions obtained. So, in the first step, the problem was to obtain from experimental data (Tables I–IV) not only the parameters $(eqQ)^v, \ldots, (eqQ)^4\cdot\eta$ but also the "centers" of multiplets $\nu_B, \ldots, \nu_F$ as well.

The problem was solved using the weighted least-squares fitting method. The hyperfine parameters and 2σ statistical confidence intervals for them are presented in Table V. To examine the correctness of the parameters obtained, calculated values are presented in Tables I–IV together with the experimental data (it should be noted that the line centers of the transitions $J = 3$ ($F' = \frac{3}{2} \leftarrow F = \frac{3}{2}$) and $J = 3$ ($F' = \frac{7}{2} \leftarrow F = \frac{7}{2}$) from Table III were not used as the initial data in the fitting). The changes in assignments of the lines $J = 7$ in Table III in comparison with those of Ref. (*7*) are the consequence of strong Coriolis interaction. The "centers" of quadrupole multiplets, which have been obtained in the analysis, are presented in Table VI.

It should also be noted that the discrepancy between the experimental and calculated data can be seen for the transitions $K = 3 \leftarrow 1$, $\Gamma = E$ ($J = 5, 6, 7$) in Table II. For $F = J \pm \frac{3}{2}$ the experimental frequencies are larger and for $F = J \pm \frac{1}{2}$ they are smaller in magnitude than the calculated values. Such a situation can easily be understood if one uses the general formula (2). One can see in this case that the frequencies of transitions $K = 3 \leftarrow 1$ can be written in the form $\sim f(\frac{3}{2}), F, J)\cdot\varphi(eqQ, \chi_J, \chi_K, \chi_d)$, where the second term does not depend practically on the quantum number J for $J = 5, 6, 7$. The Casimir function $f(\frac{3}{2}, F, J)$ ($J = 5, 6, 7$) satisfies the condition

TABLE V

Hyperfine Constants for the (0100) and (0001) Vibrational States of AsH_3 (in MHz)[a]

	(0100)	(0001)
eqQ	-161.9783(938)	-159.5228(240)
x_J	-0.1197(348)	-0.0797(127)
x_K	-0.1156(110)	-0.1481(425)
x_d	0.1375(211)	0.1045(130)
C_N	0.10662(111)	0.12089(52)
C_K-C_N	0	0
$\eta \cdot eqQ$		-1.6213(51)

[a] Values in parentheses are 2σ statistical confidence intervals.

$f(\frac{3}{2}, F, J) < 0$ for $F = J \pm \frac{1}{2}$ and $f(\frac{3}{2}, F, J) > 0$ for $F = J \pm \frac{3}{2}$. So, the regular discrepancy mentioned earlier can be removed by a simple changing of the value of $\varphi(eqQ, \chi_J, \chi_K, \chi_d)$ to 0.5–0.7 MHz. It can be made by adding a new parameter which describes the rotational dependence of the quadrupole coupling constant $(eqQ)^4$ (for example, $\chi_{KJ}J(J+1)K^2$, $\chi_{JJ}J^2(J+1)^2$, or $\chi_{KK}K^4$) to the first term of the expression $W_v^{\pm}$ (Eq. (2)). However, in this case the inverse problem stability is decreased (in particular, the confidence intervals for the parameters are increased). For this reason, and taking into account the fact that the calculated frequencies agree with the measured values within the experimental accuracy in spite of the discrepancy mentioned, the values $W_v^{\pm}$ from expression (2) were used in our analysis.

It should also be noted that the parameters C_K^v in Table VII have been used for the parameters C_N^v. The reason for this is as follows. As the analysis of the data from Refs. (*6, 7, 12, 13, 19*) has shown, the differences $|C_N^v - C_K^v|$ are very small (at most they are not larger than 20–30 kHz). So, the values of energies and line centers, in our case, depend very slightly on variations of $(C_N^v - C_K^v)$. In fact, for small values of the quantum number J (see Table I and Table III for $J = 1, 2, 3$) the values $[F(F+1) - I(I+1) - J(J+1)]$ are small and either $K = 0$ or the ratios $K^2/J(J+1)$ are small. When $J \sim 7$–8 the values $[F(F+1) - I(I+1) - J(J+1)]$ may be large enough, but, in this case, the ratios $K^2/J(J+1)$ (see Tables II and III for $J = 6, 7, 8$) are small. When $K \sim J$ (see Table IV) the contributions to the line center frequencies from the corresponding terms are not larger, as the analysis shows, than $5(C_K^v - C_N^v)$. For these reasons, the parameters $(C_K^v - C_N^v)$ in our case are poorly determinable and have been fixed at $(C_K^v - C_N^v) = 0$.

The second step of the analysis included a more accurate definition of rotational, centrifugal, and resonance parameters of the interacting states (0100) and (0001) than that in Ref. (*2*). It should be noted that the calculations based on the parameters of Ref. (*2*) can sometimes give discrepancies from the "experimental centers" of multiplets (see Table VI) up to several megacycles per second. In fact, the accuracy of infrared

TABLE VI

Centers of Quadrupole Multiplets Which Were Obtained from Analyzing the Quadrupole Splitting in the (0100) and (0001) Vibrational States of the AsH_3 Molecule

Upper State	Lower State	From Fitting (Exp.), in MHz	Calc., in MHz	E.–C., in KHz
		(0100)		
$10A_2$	$00A_1$	214757.929	214757.931	- 2
21E	11E	429599.997	429600.031	- 34
$20A_1$	$10A_2$	429671.432	429671.443	- 11
		(0001)		
$11A_2$	$11A_1$	9772.166	9772.085	81
$21A_1$	$21A_2$	29061.074	29060.932	142
$31A_2$	$31A_1$	57380.650	57380.715	- 65
$61A_1$	$61A_2$	188858.915	188858.913	2
10E	00E	230594.156	230594.011	145
$71A_2$	$71A_1$	244526.783	244526.809	- 26
$81A_1$	$81A_2$	303315.693	303315.737	- 44
53E	51E	323420.848	323420.911	- 63
83E	80E	328959.136	328959.142	- 6
63E	61E	346615.111	346615.125	- 14
82E	80E	350512.382	350512.460	- 78
73E	71E	380801.563	380801.699	-136
21E	11E	461255.368	461255.140	228
$21A_1$	$11A_2$	470511.588	470511.946	-358

experimental data, which were used for obtaining the fine structure parameters in Ref. (*2*), is 50–100 times worse than that of millimeter and submillimeter measurements (and, as a consequence, worse than the accuracy of multiplet "centers" in Table VI). Therefore, the data from Table VI with the weights 10 000 and the infrared data from Ref. (*2*) were used as the initial information for a more accurate determination of the fine structure parameters. The parameters obtained and the 2σ statistical confidence intervals for them are presented in Table VII. These parameters reproduce the infrared data (*2*) no worse than the parameters of Ref. (*2*). Reproduction of millimeter and submillimeter multiplet "centers" is presented in Table VI.[1]

The third step of our analysis consisted in repeating the procedure described above for making corrections to the parameters obtained.

[1] For the multiplet "centers" in Table VIII calculations have been made with the parameters of Ref. (*2*) only, because the differences between the calculations with the parameters of Ref. (*2*) and our parameters are much smaller than the experimental accuracy for the lines of Table VIII.

TABLE VII

Spectroscopic Constants for the (0100) and (0001) Vibrational States of AsH_3[a,b]

Constant	Value	Constant	Value
ν_2	906.7519229(1570)	$\tau_{4J}10^7$	2.4842(2101)
B_2	3.7394250(1510)	$\tau_{4JK}10^7$	-2.1931(2156)
C_2	3.52615634(2576)	$c_{11}^{(1)}$	1.9354692(9440)
$D_J^2 10^5$	9.94959(2194)	$c_{11}^{(2)}10^3$	5.95892(6591)
$D_{JK}^2 10^4$	-1.34150(1176)	$c_{11}^{(3a)}10^4$	-1.63792(1553)
$D_K^2 10^4$	1.25583(1085)	$c_{11}^{(3b)}10^5$	4.3802(4059)
$H_J^2 10^9$	5.8722(2883)	$c_{21}^{(2)}10^2$	1.43897(2026)
$H_{JK}^2 10^8$	-1.4449(1758)	$c_{21}^{(3)}10^5$	-8.198(1600)
$H_{KJ}^2 10^8$	1.1184(1479)	$c_{21}^{(4a)}10^7$	-3.156(2109)
$H_K^2 10^9$	5.3849(6956)	$c_{21}^{(4b)}10^6$	6.2002(9177)
ν_4	999.2244145(1007)	$q_{22}^4 10^3$	-1.38409(3744)
B_4	3.76575822(8391)	f_{22}^{4J}	0.0
C_4	3.48041557(2554)	$f_{22}^{4K}10^7$	6.715(3643)
$D_J^4 10^4$	1.0201294(8879)	$q_{12}^4 10^2$	-1.44166(1647)
$D_{JK}^4 10^4$	-1.307497(3427)	$f_{12}^{4J}10^6$	5.7019(6382)
$D_K^4 10^4$	1.142518(3919)	$f_{12}^{4K}10^7$	-9.643(4540)
$H_J^4 10^9$	8.0495(1344)	$f_{42}^4 10^8$	3.902(4876)
$H_{JK}^4 10^8$	-1.38509(6268)	$\varepsilon^2 10^5$	2.8213(1505)
$H_{KJ}^4 10^9$	4.4709(7818)	$\varepsilon^4 10^5$	1.89108(5984)
$H_K^4 10^9$	8.1587(4879)	$\varepsilon_J^4 10^9$	-7.193(1143)
$(c\zeta)_4$	-1.58344544(3744)	$\varepsilon_K^2 10^9$	5.448(1258)
$\eta_{4J}10^4$	-2.330552(6545)	$\varepsilon_J^4 10^9$	-0.9375(4254)
$\tau_{4K} = \eta_{4K}$	0.0	$\varepsilon_K^4 10^9$	1.2378(9471)

[a] In the calculations the parameters of the ground vibrational state have been taken from Ref. (*18*).
[b] Values in parentheses are 2σ statistical confidence intervals.

V. DISCUSSION

In the literature beginning, for example, with Ref. (*1*) and further with Refs. (*2, 6, 7, 11–13, 18, 19*), some sets are given for the parameters of the ground and excited vibrational states of the AsH_3 molecule obtained as a result of analyzing different sets of experimental data in the framework of various Hamiltonian models. The comparisons of the results obtained have shown the strong dependence of molecular parameters on experimental data as well as on the theoretical models. In particular, the use of *l*-doubling constants, given in Ref. (*7*), for describing direct *l*-type doubling transitions in the (0001) state ($J = 6, 7, 8$) differs (see Table IX) from the results of calculation

TABLE VIII

Transition Frequencies of the AsH_3 Molecule in the (0100) and (0001) Vibrational States: Allowed Transitions $J = 4 \leftarrow 3$ ($\Delta K = 0$)

Transition K Γ′ ← K Γ		Exp., MHz	Calc.(MHz) Ref.(2)	E.-C., MHz
		(0100)		
3A2	3A1	859 286	859 282.7	3.3
2E	2E	859 953	859 950.9	2.1
1E	1E	860 346	860 342.7	3.3
0A1	0A2	860 472	860 470.7	1.3
		(0001)		
0E	0E	912 591	912 635.2	-44.2
1E	1E	917 421	917 436.7	-16.1
2A2	2A1	920 128	920 107.3	20.7
2A1	2A2	920 385	920 375.0	10.0
3E	3E	922 775	922 770.3	4.7
3E	3E	924 074	924 058.8	15.2
2E	2E	928 197	928 189.4	7.6
1A1	1A2	938 614	938 629.9	-15.9

with the parameters of Ref. (*2*). Also, the discrepancies between the microwave experimental data and calculations with the parameters from Ref. (*2*) are essentially greater than the experimental accuracy of the microwave measurements.

In this paper the use of precise submillimeter-wave data, which have been recorded by a high-sensitivity optoacoustic spectrometer with quasi-optical multipass cavity absorption cells (RAD), together with the infrared and radiofrequency results, ensured an extensive and reliable basis for adequate description of the states of the AsH_3 molecule.

TABLE IX

Calculated "Center" Line Frequencies Corresponding to the Direct *l*-Type Doubling Transitions in the (0001) State of AsH_3 (in MHz)

Transition J′K′Γ′ ← JKΓ		Calc., Ref.(7)	Calc., Ref.(2)	Our Calc.	Exp.
11A2	11A1	9772.17	9771.44	9772.082	9772.166
21A1	21A2	29061.08	29058.89	29060.923	29061.074
31A2	31A1	57380.61	57377.29	57380.690	57380.650
61A1	61A2	189416.04	188854.88	188858.879	188858.915
71A2	71A1	246638.02	244525.75	244526.848	244526.783
81A1	81A2	309600.98	303318.96	303315.626	303315.693

The problem of confined analysis of all experimental data was solved by the improvement of the theoretical model for the molecule, in which the influence of Coriolis interaction on the hyperfine spectral structure was taken into account. Such consideration enabled us to obtain the set of spectroscopic parameters (see Table V) which is responsible for the description of hyperfine splittings in the (0100) and (0001) states and describes most precisely all known microwave spectra of the arsine molecule. As an illustration of what has been stated above, Table X presents the results of calculations

TABLE X

Calculated Line Frequencies (MHz) Corresponding to Some Hyperfine Transitions in the (0100) and (0001) States of AsH_3[a]

$J'K'\Gamma'F'$ ←	$JK\Gamma F$	Calc. Ref.(7)	Calc. Ref.(11)	Calc. Ref.(13)	Calc. Ref.(19)	Our Calc.	$\nu_{exp.}-\nu_0$
				(0100)			
$10A_2$ 3/2	$00A_1$ 3/2	-	-32.07	-32.70	-	-32.07	-32.08
5/2	3/2	-	8.14	8.31	-	8.15	8.14
1/2	3/2	-	39.72	40.46	-	39.69	39.72
$20A_1$ 5/2	$10A_2$ 5/2	-	-36.73	-37.46	-	-36.83	-37.09
5/2	3/2	-	3.47	3.59	-	3.39	3.58
7/2	5/2	-	3.57	3.66	-	3.62	3.58
3/2	3/2	-	31.77	32.37	-	31.75	31.86
55E 11/2	55E 9/2	-	17.446	17.480	-	17.489	17.475
11/2	13/2	-	59.305	59.233	-	59.231	59.240
9/2	7/2	-	60.383	60.390	-	60.405	60.406
				(0001)			
10E 3/2	00E 3/2	-31.98	-31.96	-32.29	-32.30	-31.97	-31.98
5/2	3/2	8.15	8.12	8.21	8.21	8.14	8.12
1/2	3/2	39.50	39.54	39.94	39.96	39.51	39.53
55E 11/2	55E 9/2	17.396	17.439	17.101	17.123	17.382	17.388
11/2	13/2	58.486	59.019	58.648	58.561	58.487	58.486
83E 13/2	80E 13/2	-11.32	- 8.96	- 9.00	- 9.03	-12.07	-12.17
19/2	19/2	- 7.95	- 6.29	- 6.43	- 6.42	- 8.48	- 8.45
15/2	15/2	7.55	5.97	6.08	6.08	8.06	8.09
17/2	17/2	10.92	8.64	8.74	8.75	11.66	11.65
$11A_2$ 5/2	$11A_1$ 5/2	- 0.11	0.0	0.0	0.0	- 0.12	- 0.11
1/2	3/2	-35.94	-35.99	-36.30	-36.32	-35.95	-35.97
5/2	3/2	-19.36	-19.63	-19.86	-19.87	-19.35	-19.33
3/2	5/2	19.69	19.63	19.86	19.87	19.72	19.66
$81A_1$ 13/2	$81A_2$ 13/2	- 0.33	0.0	0.0	0.0	- 3.02	- 2.99
19/2	19/2	- 0.23	0.0	0.0	0.0	- 2.10	- 2.17
15/2	15/2	0.22	0.0	0.0	0.0	2.00	2.10
17/2	17/2	0.32	0.0	0.0	0.0	2.88	2.84

[a] For convenience, not the values of line frequencies ν but the values of differences $(\nu - \nu_0)$ are presented in Table X. Here ν_0 are the centers of quadrupole multiplets from column 3 of Table VI.

made in the framework of different Hamiltonian models with various sets of parameters (*7, 11, 13, 19*) of some hyperfine transition energies from Tables I–IV. The experimental data and the results of our calculation are also presented in Table X. It can be seen that the parameters and models from Refs. (*7, 11, 13, 19*), which describe satisfactorily one set of experimental data, as a rule, describe the data from other spectra unsatisfactorily. At the same time, the parameters presented in this paper describe all known experimental data satisfactorily.

It should also be noted that the significant increase of the experimental information, as compared with the data available previously in the literature, allowed us to determine not only the usual parameters (see (*7, 11, 13, 19*)) but also some parameters from Eq. (2), which were not evaluated previously.

The use of precise submillimeter and radiofrequency data with sufficiently large values of the quantum numbers J and K enabled us to improve not only hyperfine parameters but also the rotational, centrifugal, and resonance parameters. The data of Table IX can serve as an example of what has been said above.

Thus, it should be stated that, as a result of the combined analysis of new submillimeter-wave data together with the known infrared, microwave, and radiofrequency measurements, the set of spectroscopic parameters obtained allowed us to describe all the available spectroscopic data for the (0100) and (0001) vibrational states of the AsH_3 molecule within the measurement accuracies.

RECEIVED: October 23, 1986

REFERENCES

1. K. SARKA, D. PAPOUSEK, AND K. NARAHARI RAO, *J. Mol. Spectrosc.* **37**, 1–19 (1971).
2. G. DILONARDO, L. FUSINA, AND J. W. C. JOHNS, *J. Mol. Spectrosc.* **104**, 282–301 (1984).
3. S. URBAN, V. SPIRKO, D. PAPOUSEK, R. S. MCDOWELL, G. NERESON, S. P. BELOV, L. I. GERSHTEIN, A. V. MASLOVKSY, A. F. KRUPNOV, J. CURTIS, AND K. NARAHARI RAO, *J. Mol. Spectrosc.* **79**, 455–495 (1980).
4. S. P. BELOV, A. V. BURENIN, L. I. GERSHTEIN, A. F. KRUPNOV, V. N. MARKOV, A. V. MASLOVSKY, AND S. M. SHAPIN, *J. Mol. Spectrosc.* **86**, 184–192 (1981).
5. National Bureau of Standards, "Microwave Spectral Tables," Vol. 4, No. 3, Washington, D.C., 1968.
6. A. V. BURENIN, V. P. KAZAKOV, A. F. KRUPNOV, A. A. MELNIKOV, AND S. M. SHAPIN, *J. Mol. Spectrosc.* **94**, 253–263 (1982).
7. F. SCAPPINI, G. DILONARDO, A. GUORNIERI, A. F. KRUPNOV, AND V. P. KAZAKOV, *J. Mol. Spectrosc.* **112**, 377–383 (1985).
8. V. P. KAZAKOV, *Izv. Vyssh. Uchebn. Zaved. Radiofiz.* **23**, 877–979 (1980).
9. V. P. KAZAKOV, V. V. PARSHIN, AND YU. A. DRIAGIN, *Izv. Vyssh. Uchebn. Zaved. Radiofiz.* **29**, 240–243 (1986).
10. A. F. KRUPNOV, *Vestn. Acad. Nauk SSSR* **7**, 18 (1978).
11. V. P. KAZAKOV AND A. A. MELNIKOV, *Izv. Vyssh. Uchebn. Zaved. Radiofiz.* **28**, 379–382 (1985).
12. D. A. HELMS AND W. GORDY, *J. Mol. Spectrosc.* **69**, 473–481 (1978).
13. F. SCAPPINI AND T. OKA, *J. Mol. Spectrosc.* **85**, 390–398 (1981).
14. W. GORDY AND R. L. COOK, "Microwave Molecular Spectra," Interscience, New York, 1970.
15. J. T. HOUGEN, *J. Chem. Phys.* **57**, 4207–4217 (1972).
16. G. TARRAGO AND S. MAES, *C.R. Acad. Sci. Paris* **266**, 699–702 (1968).
17. E. ARIMONDO, P. GLORIEUX, AND T. OKA, *Phys. Rev. A* **17**, 1375–1393 (1978).
18. M. CARLOTTI, G. DILONARDO, AND L. FUSINA, *J. Mol. Spectrosc.* **102**, 310–319 (1983).
19. F. SCAPPINI, L. FUSINA, AND G. DILONARDO, *J. Mol. Spectrosc.* **107**, 419–420 (1984).
20. T. OKA, *J. Chem. Phys.* **47**, 5410–5426 (1967).